

# Response of *Bacillus thuringiensis* Al Hakam Endospores to Gas Dynamic Heating in a Shock Tube

By A. Daniel McCartt<sup>1,\*,#</sup>, Sean D. Gates<sup>1,#</sup>, Jay B. Jeffries<sup>1</sup>, Ronald K. Hanson<sup>1</sup>, Lydia M. Joubert<sup>2</sup>, and Tony L. Buhr<sup>3,#</sup>

<sup>1</sup> Mechanical Engineering Department, Stanford University, Building 520, 452 Escondido Mall, Stanford, CA, 94305-3032, USA

<sup>2</sup> Cell Sciences Imaging, Stanford Medical School, Stanford University, Stanford, CA, 94305, USA

<sup>3</sup> Naval Surface Warfare Center-Dahlgren, Dahlgren, VA 22448, USA

*Dedicated to Katharina Kohse-Höinghaus on the occasion of her 60<sup>th</sup> birthday*

(Received September 8, 2011; accepted in revised form November 11, 2011)

## *Bacillus* Endospores / Flow Cytometry / Shock Wave Heat Resistance / Laser Diagnostics / Scanning Electron Microscopy

Experiments were conducted in a gas-driven shock tube to investigate shock wave-induced damage to *Bacillus thuringiensis* Al Hakam endospores over a wide range of post-shock temperatures in non-oxidative gas environments. The results were compared with previous studies on *B. atrophaeus* and *B. subtilis* and demonstrate that *B. thuringiensis* Al Hakam exhibited a qualitatively similar response to rapid shock heating, even though this strain has a significantly different endospore structure. *B. thuringiensis* Al Hakam endospores were nebulized into an aqueous aerosol, which was loaded into the Stanford aerosol shock tube, and subjected to shock waves of controlled strength. Endospores experienced uniform test temperatures between 500 and 1000 K and pressures ranging from 2 atm to 7 atm for approximately 2.5 ms. During this process the bio-aerosol was monitored using *in situ* time-resolved laser absorption and scattering diagnostics. Additionally, shock-treated bio-aerosol samples were extracted for *ex situ* analysis including viability plating, flow cytometry and scanning electron microscopy (SEM) imaging. *B. thuringiensis* Al Hakam endospores lost the ability to form colonies at post-shock temperatures above 500 K while significant breakdown in morphology was observed only for post-shock temperatures above 700 K. While viability loss and endospore morphological deterioration adhere to a similar framework across all endospore species studied, phenomena unique to *B. thuringiensis* Al Hakam were noted in the SEM images and optical extinction data. This initial characterization of the response of *B. thuringiensis* Al Hakam spores treated with shock/blast waves shows that these methods have potential for spore inactivation and detection.

## 1. Introduction

In response to environmental stress, gram-positive *Bacillus* species can activate a complex process of genetic, biochemical and morphological events that lead to sporulation

\* Corresponding author. E-mail: mccartt@stanford.edu

# Authors contributed equally to this work.

and the development of a metabolically dormant endospore. Endospores are comprised of a series of nested proteinaceous shells that protect the core of the endospore. The core contains cellular essentials that return the dormant endospore to a vegetative state once the environment is more favorable. Endospores are characterized by increased resilience to a variety of deleterious treatments including chemical agents, high temperatures, and UV radiation; the dehydrated endospore is a unique and extremely durable biological entity [1–3].

In an attempt to extend the understanding of endospore response to stress mechanisms we have developed a laboratory protocol to study the biological and structural breakdown of aqueous aerosols of endospores exposed to shock heating [4]. The endospores, suspended in an aqueous aerosol, are introduced into the test section of a gas-driven shock tube developed for combustion chemistry [5] and this spore-laden aerosol is subjected to shockwaves of controlled strength. *In situ* endospore structural decomposition is monitored with scattering from intact endospores and absorption by endospore biochemicals using time-resolved laser-extinction measurements at 665 nm and 266 nm respectively. Pre- and post-shock samples are extracted from the test region with the use of a gas-dynamic liquid impinger and undergo *ex situ* analysis to assess loss of viability and morphological deterioration. Quantitative measurements of shock-treated endospore viable fraction are ascertained via a combination of standard agar plating techniques and flow cytometry. In addition to enumerating the shock-treated endospores, flow cytometer analysis is utilized to monitor endospore morphological degradation through the use of a nucleic-acid-binding dye. Qualitative assessment of endospore morphology is performed utilizing scanning electron microscopy.

Our previous studies of the response of *B. atrophaeus* and *B. subtilis* to shock waves in an inert and an oxidative gas environment indicated three distinct stages of shock wave-induced endospore damage with inactivation occurring before the onset of significant morphological deterioration. In this manuscript results are presented for shock wave-treated spores of *B. thuringiensis* Al Hakam. This strain was chosen because it was isolated from a suspected weapons of mass destruction facility in Iraq [6], and it better simulates the threat agent *B. anthracis* [7–11] but is thought to be safe for general research [12]. In contrast to endospores of *B. atrophaeus* and *B. subtilis* studied in previous experiments, *B. thuringiensis* endospores are larger, possess a thin cell coat, and display an architectural network composed of a crystalline hexagonal honeycomb mesh encased in a flexible exosporium. The exosporium interacts with the environment and confers significant hydrophobicity to spores [13–22]. One might speculate that this exosporium provides resistance to the rapid heating and short high-temperature test time behind a shock wave. The viability and morphological composition of *B. thuringiensis* Al Hakam spores was examined after exposure to shock-heated flows.

## 2. Experimental

### 2.1 Stanford aerosol shock tube

The experimental method employed in the present study was detailed in our previous work, therefore only a brief summary will be provided [4]. All experiments were con-

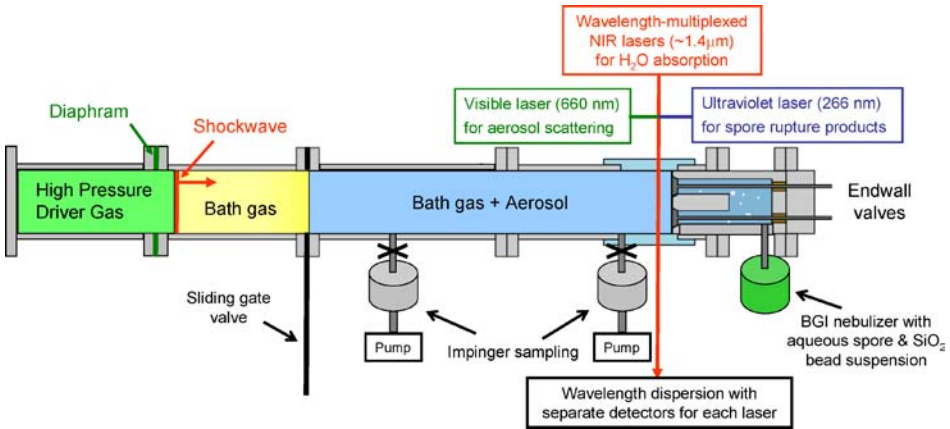


**Fig. 1.** Schematic of the SAST facility configured for shock-heating spore-laden aerosols. Three *in situ* laser diagnostics monitor the shock-heated gas/aerosol, while pre- and post-shock samples are taken with gas dynamic impingers for *ex situ* analysis. (Not drawn to scale).

ducted using the Stanford aerosol shock tube (SAST) [5]. The SAST consists of a driver and a driven section separated by a thin diaphragm as illustrated in Fig. 1. The driven section is further divided by a sliding gate valve into an upstream section and a test section. During preparation for a test the upstream region is filled with the test bath gas and the test section is filled with a mixture of test bath gas and bioaerosol produced by a pneumatic nebulizer. Before each test a pre-shock sample is collected with an impinger for *ex situ* analysis. After extracting the pre-shock sample, the gate valve is opened and the driver section is filled with Helium gas until the diaphragm ruptures. This event produces a planar shock wave that propagates into the driven section. Upon arrival of the incident shock the gas/bioaerosol mixture at initial temperature and pressure  $T_1$  and  $P_1$  is rapidly heated and compressed to  $T_2$ ,  $P_2$ . Subsequent reflection of the shock wave by the endwall heats and compresses the mixture a second time to the test conditions  $T_5$  and  $P_5$ . In this region the flow is stagnated and the test conditions persist for 2–3 ms followed by rapid cooling. Immediately following the shock events, the sliding gate valve is returned to the closed position and a sample is collected with the post-shock impinger.

## 2.2 Endospore suspension, loading, and sampling

Endospores of *B. thuringiensis* Al Hakam were prepared in 0.8% nutrient broth (NB) amended with CCY salts [20]. Sterile-filtered, refined olive oil (Sigma O1514) was added as a non-toxic anti-foam to a final concentration of 5%. Sporulation was performed in 333 mL of pre-aerated broth contained in 1-L plastic baffled flasks (Corning® Part No. 431403) and incubated in New Brunswick Scientific shaker/incubators at 34 °C, 300 rev min<sup>-1</sup> for 72±2 h. Spores were pelleted at 2000 g, 4 °C for 10 min. Spore pellets were re-suspended and washed 4 times with sterile-filtered 5% Tween 80 (Sigma P1754), suspended in 33.3 mL of 0.1% Tween 80, and frozen at -80 °C. Samples were removed at various times after sporulation and heat-

treated at 65 °C for 30 min to determine viable spore titers. Samples were serially diluted in 0.1% Tween 80, pH7, and dilutions were used to inoculate tryptic soy agar (TSA) plates acquired from Remel. Plates were incubated for  $16 \pm 1$  h at 37 °C prior to colony counting. Heat-resistant titers for independent spore preparations ranged from  $2.3\text{--}8.9 \times 10^5$  spores mL<sup>-1</sup> after cold storage. Light microscopy showed 80–95% phase-bright spores with the remainder being dead, decaying vegetative cells. Finally, 1 µm SiO<sub>2</sub> beads are added to the suspension. These beads act as an indestructible tracking particle, remaining physically undisturbed for all post-shock temperatures below 1400 K.

The aqueous bioaerosol was produced from the *B. thuringiensis* Al Hakam endospore suspension with a gas dynamic nebulizer (6-jet Collison type, BGI Inc.). Endospores were loaded into the shock tube in an Argon carrier gas. Samples for *ex situ* analysis were vacuum extracted from the test section of the SAST before and after the shock event with commercial (Ace Glass Inc.) gas dynamic liquid impingers. The aerosol flow through the impinger is directed onto a 10 ml pool of filtered, sterilized water where particulates in the flow are deposited. Neither the nebulization nor the vacuum extraction process adversely affected the viability or morphological structure of the *B. thuringiensis* Al Hakam endospores. Further details concerning this method can be found in Gates *et al.* 2010.

### 2.3 *Ex situ* analysis

100 µL samples from a series of dilutions of the pre- and post-shock impinger samples were plated on nutrient agar (NA) plates for viable counts. Following overnight incubation at 29 °C colonies were counted. Colony count stabilization was ensured through continued incubation at room temperature for another 48 h. Each sample was plated five times, at five different dilutions.

Flow cytometry measurements were conducted to enumerate the particles in the pre- and post-shock impinger samples and to monitor for morphological damage resulting from exposure to shock-heated flows. A four-laser BD Biosciences, model LSR II with laser excitation at 405, 488, 532 and 635 nm was employed. Endospore resistance to shock exposure is quantified by combining the results of the plating and flow cytometer analysis. These results are subsequently used to generate the viable fraction; a measure of the amount of initially viable spores that remain viable after shock-exposure. A detailed discussion of this quantity and how it is computed can be found in Gates *et al.* 2010.

Coupled with the aforementioned quantification techniques, an additional qualitative method, scanning electron microscopy (SEM) was employed to assess pre- and post-shock endospore morphological structure. The SEM employed in this study was the Hitachi model S-3400N VP. Interrogation samples are filtered (0.22 µm cellulose, Millipore, MA), air-dried, and placed on double-sided carbon tape on aluminum stubs (Electron Microscopy Sciences, PA). Stubs were subsequently sputter-coated (100 Å layer) with gold-palladium in a Denton Vacuum Desk II unit. Sample visualization was then preformed utilizing secondary electron detection with the SEM, operated under high vacuum at 10 and 15 kV at a working distance of 8–9 mm. Images (2560 × 1920 pixels) were captured with a CCD camera.

## 2.4 *In situ* analysis

Laser diagnostics have been employed extensively to make non-intrusive measurements in shock-heated flows [23]. These techniques were utilized in the present study to measure the real-time evolution of endospore morphological damage *in situ*. A cursory overview of the *in situ* diagnostics and analysis is provided here. For a detailed discussion please refer to McCartt *et al.* 2011 [24].

Real-time optical extinction measurements at 266 nm and 665 nm are used to monitor the evolution of the bioaerosol shock-wave interaction. The UV light at 266 nm is both strongly absorbed by UV-active endospore biochemicals (*e. g.* dipicolinic acid and nucleic acids) and scattered by intact endospores. The visible light at 665 nm, however, is only scattered by the bioaerosol. Consequently, by monitoring the post-shock decay of the 665 nm extinction signal we are able to measure a time history of endospore structural decomposition. Furthermore, the UV light at 266 nm corroborates the 665 nm signal by monitoring the release of biochemicals from endospore decomposition and lysis. For low to moderate post-shock temperatures ( $T_5$ ) endospores remain largely intact and both laser extinction signals undergo step changes in magnitude as the shock waves pass through the measurement location. For high-temperature cases, however, decay in the visible optical extinction signal indicates endospore morphology degradation, while the elevated level of 266 nm optical extinction signifies the presence of released UV-active biochemicals.

Multiplexed fiber-coupled lasers tuned to two near-infrared (NIR) water vapor absorption transitions are used to determine time-resolved gas temperature of the water vapor in the bioaerosol. Water vapor transitions are chosen near 1343.3 and 1391.7 nm, with lower-state energy values of 1790 and 1045  $\text{cm}^{-1}$  respectively. Each of the lasers is scanned in wavelength over the absorption feature. Rapid scanning of the laser wavelengths provides integrated absorption line strengths for each transition with 50  $\mu\text{s}$  time resolution. The water vapor temperature is used in conjunction with the shock speed to determine post-shock temperature.

## 3. Results

### 3.1 *B. thuringiensis* Al Hakam response to shock-heated flows

A measurement campaign was conducted to examine the response of *B. thuringiensis* Al Hakam to shock-heated flows. Using the procedures and protocols detailed above, the shock-wave bioaerosol interaction was monitored with *in situ* optical diagnostics, and pre- and post-shock endospore suspensions were subjected to *ex situ* examination including: agar plating viability analysis, flow cytometer quantification, and scanning electron microscopy imaging.

Performing experiments with an endospore species differing in structural composition from those previously studied allows us to determine if the rate of viability reduction and morphological breakdown as a function of post-reflected shock temperature is a feature largely independent of physical constitution. The shock heating is quite rapid and the test time at the post-shock temperature is only a few milliseconds leading to speculation that the exosporium of *B. thuringiensis* Al Hakam would provide en-

hanced resistance to this rapid heating compared to the long time (equilibrium heating) applied in more standard heat resistance studies.

### 3.1.1 Scanning electron microscopy

Pre- and post-shock sample analysis was conducted utilizing scanning electron microscopy imaging. Representative data is presented in Fig. 2 below. Image a) consists of untreated *B. thuringiensis* Al Hakam endospores collected from the nebulizer. The presence of the loose-fitting exosporium is readily apparent. The second image, b), is of a nebulized pre-shock sample extracted from the shock tube through the gas dynamic impinger. The exosporium and overall structure of the endospore remain intact and uncompromised. The morphological effect of exposure to a shock wave generating a  $T_5$  of 500 K is demonstrated in image c). As was found in previous studies, the post-shock samples of low temperature experiments exhibit virtually no morphological deterioration. In addition, intact exosporiums are clearly visible. With increased post-shock temperatures, however, the onset of structural deterioration becomes apparent. Image d) illustrates the effect of endospore exposure to a post-shock temperature of 630 K. While the overall structure of the endospore remains intact the exosporium is absent and prominent morphological changes have become apparent.

### 3.1.2 Viable fraction

To further elucidate the response of *B. thuringiensis* Al Hakam to shock heated flows viability analysis of pre- and post-shock samples was performed. Figure 3 plots *B. thuringiensis* Al Hakam viability results along with data from previous *B. atrophaeus* and *B. subtilis* tests in the same inert gas environment [4].

The data sets indicate an analogous trend in viability reduction between the three species. While past studies have demonstrated the consistent response of wild type endospores of related species sharing similar structural compositions [25], the data illustrated in Fig. 3 indicates that this characteristic viability reduction response can be applied to species with significantly different physical constitutions. Even for the 530 K test where the SEM indicates the exosporium remains intact, the exosporium of *B. thuringiensis* Al Hakam did not provide increased thermal resistance to viability loss from the rapid shock heating. This hypothesis is furthered reinforced by examining the *in situ* optical measurements.

### 3.1.3 Laser diagnostics

*In situ* optical diagnostics were employed to monitor the real time response of *B. thuringiensis* Al Hakam endospores to shock heating. The 665 nm optical time histories for relatively weak ( $T_5 = 500$  K) and strong ( $T_5 = 990$  K) shocks are plotted in Figs. 4 and 5 below. Step changes in extinction correspond to discrete jumps in density across the incident and reflected shock waves. Using the shock-jump relations and region 2 extinction values, the extinction in region 5 can be predicted [26]. The predicted extinctions are represented by dotted lines in Figs. 4 and 5. For the relatively weak shock (Fig. 4  $T_5 = 500$  K), measured and predicted values agree, and extinction remains relatively constant during region 5. This indicates minimal endospore morphology breakdown for this low-temperature condition.

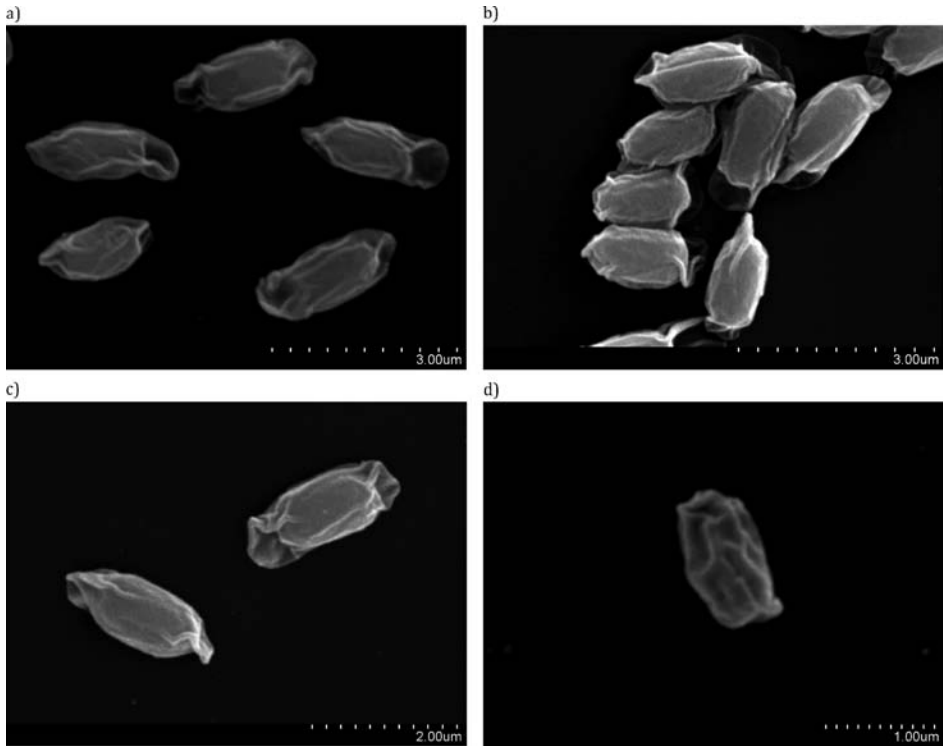


**Fig. 2.** Scanning Electron Microscopy (SEM) images: a) Untreated nebulizer sample; b) Pre-shock sample; c) Post-shock sample with  $T_5 = 500$  K; d) Post-shock sample with  $T_5 = 630$  K.

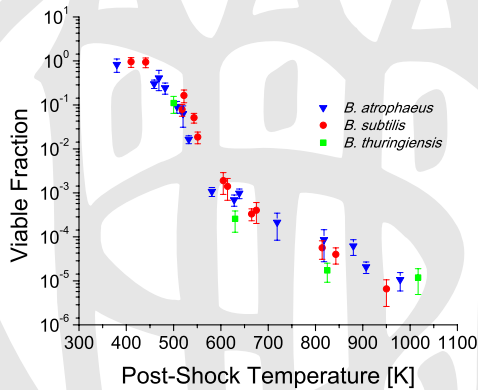


**Fig. 3.** Viable fraction plotted vs. post-reflected shock temperature ( $T_5$ ) for a test time of approximately 2.5 ms. Triangle: *B. atrophaeus*; circle: *B. subtilis*; square: *B. thuringiensis* Al Hakam.

In contrast, for shocks with very high temperatures (e. g. Fig. 5  $T_5 = 990$  K) all of the endospores are destroyed, and the visible scattering at long time arises solely from  $\text{SiO}_2$  bead scatter. In previous experiments with *B. atrophaeus* and *B. subtilis*, an initial

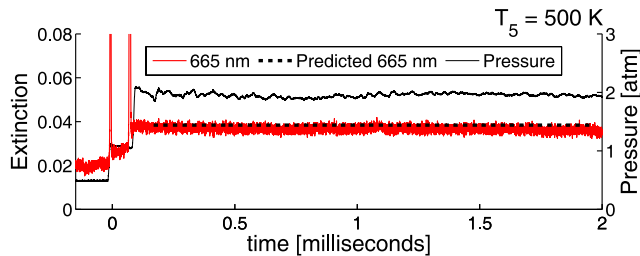


**Fig. 4.** Extinction plotted vs. time for *in situ* diagnostics at 665 nm (red) for low temperature shock ( $T_5 = 500$  K). No decay is seen in region 5. Step changes in extinction correspond to density jumps across shock waves. The predicted extinction values (dotted line) are calculated with shock jump equations and region 2 extinction values.

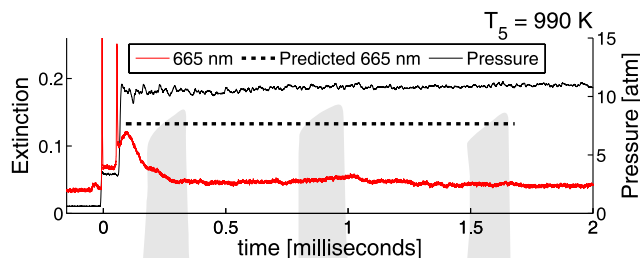


**Fig. 5.** Extinction plotted vs. time for *in situ* diagnostics at 665 nm (red) for a high temperature shock ( $T_5 = 990$  K). Endospore breakdown is observed by decreasing region 5 665 nm scatter. The predicted extinction values (dotted line) are calculated with shock jump equations and region 2 extinction values.

short-term rise in extinction above the expected level was observed. The initial breakup of intact endospores was hypothesized to decrease the individual volume of endospore particulate but briefly increase the total scattering cross-section. This phenomenon is also detected in *B. thuringiensis* Al Hakam tests (as seen in Fig. 5). However in contrast to previous experiments with other species, extinction levels remain at or below the expected level. This observation suggests that some morphological damage is occurring during the passage of the reflected shock; possibly the partial or complete removal of the exosporium.

Pertinent data regarding the structural integrity of the endospore is extracted from the long time 665 nm extinction signal levels. Specifically, the fraction of endospores that remain intact as a function of post-shock temperature ( $T_5$ ) is quantified and shown in Fig. 6. Similar to other experiments with *B. atrophaeus* and *B. subtilis* endospores, the rate of structural decomposition is rapid between 700 and 900 K. For all species, minimal morphological damage is incurred for tests with  $T_5$  below 700 K, while complete morphological deterioration is observed for experiments with  $T_5$  greater than 900 K.

In addition to the 665 nm laser, a 266 nm laser was utilized to monitor the release of UV active biochemicals from ruptured endospores. Previous studies with *B. atrophaeus* and *B. subtilis* have indicated the level of 266 nm laser extinction consistently increases as endospore deterioration commences due to the rapid dispersion of absorb-



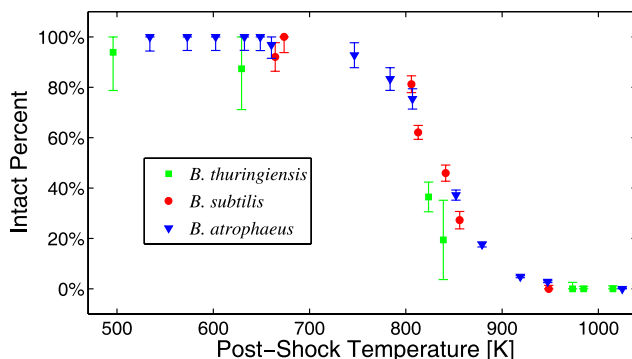


**Fig. 6.** Percentage of endospores morphology that remains intact after the high temperature region 5 test time plotted vs. post-shock temperature ( $T_3$ ). Triangle: *B. atrophaeus*; circle: *B. subtilis*; square: *B. thuringiensis* Al Hakam.

ing lysate molecules [24]. The *B. thuringiensis* Al Hakam experiments in this study, however, deviated significantly from this trend. Ultra violet extinction at long times for high temperature shocks was reduced and somewhat inconsistent (data not shown). Further experimentation is necessary to determine the physical mechanisms behind the observed 266 nm post-shock extinction.

#### 4. Discussion

Previous experiments showed that *B. atrophaeus* and *B. subtilis* endospores exhibited a three-tiered response to gas dynamic heating [4,25]. *B. thuringiensis* Al Hakam endospores adhered to this framework suggesting that structural differences among these species provide negligible difference in resistance to gas-dynamic heating.

*Ex situ* analysis indicates that *B. thuringiensis* Al Hakam viability response to gas dynamic heating is similar to previously tested species, and that for the short-time exposure to the high post-shock temperatures studied here, the exosporium structure does not provide added resistance to heat treatment. The majority of endospore viability loss occurred by internal disruption of biochemical networks critical for agar plate colony formation, with a four log reduction in viable fraction occurring before the onset of significant morphological damage.

While the survival kinetics of *B. thuringiensis* Al Hakam endospores after gas dynamic heating followed the same overall trend as *B. atrophaeus* and *B. subtilis*, several phenomena unique to this species were observed. SEM analysis of post-shock samples from the 630 K shock showed evidence of endospores stripped of their exosporia. Furthermore, for the dynamic range (700–900 K) Fig. 6 shows a slightly increased amount of morphological damage for *B. thuringiensis* Al Hakam endospores. It is hypothesized that this increase amount of morphological damage is due to the removal of the loose-fitting exosporium. Finally, the 266 nm extinction after disintegration of *B. thuringiensis* Al Hakam endospores was relatively reduced. The reduction in signal suggests either a dearth of biochemicals within the endospore – possibly due to differ-

ences in growth media – or reduced dispersion of UV-active biochemicals after spore rupture due to inter-species structural differences.

## Acknowledgement

We celebrate the birthday of Professor Dr. Kohse-Höinghaus. Like many examples of her research, the work here applies physical chemistry tools and laser diagnostics to solve problems in other disciplines. This work was supported by the Defense Threat Reduction Agency via grant AB07TAS014, administered by the Army Research Office under grant 51532CHCBB with Dr. Jennifer Becker of the Chemical Sciences Division as contract monitor. Alice Young and Zachary Minter at Naval Surface Warfare Center-Dahlgren provided technical assistance with the spore preparation.

## References

1. P. Setlow, *J. Appl. Microbiol.* **101** (2006) 514.
2. W. L. Nicholson, N. Munakata, G. Horneck, H. J. Melosh, and P. Setlow, *Microbiol. Mol. Biol. Rev.* **64** (2000) 548.
3. W. H. Coleman, D. Chen, Y. Q. Li, A. E. Cowan, and P. Setlow, *J. Bacteriol.* **189** (2007) 8458.
4. S. D. Gates, A. D. McCartt, P. Lappas, J. B. Jeffries, R. K. Hanson, L. A. Hokama, and K. E. Mortelmans, *J. Appl. Microbiol.* **109** (2010) 1591.
5. D. F. Davidson, D. R. Haylett, and R. K. Hanson, *Combust. Flame* **155** (2008) 108.
6. L. Radnedge, P. G. Agron, K. K. Hill, P. J. Jackson, L. O. Ticknor, P. Keim, and G. L. Andersen, *Appl. Environ. Microbiol.* **69** (2003) 2755.
7. P. M. Hauser and D. Karamata, *Biochimie* **74** (1992) 723.
8. C. S. Han, G. Xie, J. F. Challacombe, M. R. Altherr, S. S. Bhotika, D. Bruce, C. S. Campbell, M. L. Campbell, J. Chen, O. Chertkov, C. Cleland, M. Dimitrijevic, N. A. Doggett, J. J. Fawcett, T. Glavina, L. A. Goodwin, K. K. Hill, P. Hitchcock, P. J. Jackson, P. Keim, A. R. Kewalramani, J. Longmire, S. Lucas, S. Malfatti, K. McMurry, L. J. Meincke, M. Misra, B. L. Moseman, M. Mundt, A. C. Munk, R. T. Okinaka, B. Parson-Quintana, L. P. Reilly, P. Richardson, D. L. Robinson, E. Rubin, E. Saunders, R. Tapia, J. G. Tesmer, N. Thayer, L. S. Thompson, H. Tice, L. O. Ticknor, P. L. Wills, T. S. Brettin, and P. Gilna, *J. Bacteriol.* **188** (2006) 3382.
9. A. R. Hoffmaster, K. K. Hill, J. E. Gee, C. K. Marston, B. K. De, T. Popovic, D. Sue, P. P. Wilkins, S. B. Avashia, R. Drumgoole, C. H. Helma, L. O. Ticknor, R. T. Okinaka, and P. J. Jackson, *J. Clin. Microbiol.* **44** (2006) 3352.
10. J. F. Challacombe, M. R. Altherr, G. Xie, S. S. Bhotika, N. Brown, D. Bruce, C. S. Campbell, M. L. Campbell, J. Chen, O. Chertkov, C. Cleland, M. Dimitrijevic, N. A. Doggett, J. J. Fawcett, T. Glavina, L. A. Goodwin, L. D. Green, C. S. Han, K. K. Hill, P. Hitchcock, P. J. Jackson, P. Keim, A. R. Kewalramani, J. Longmire, S. Lucas, S. Malfatti, D. Martinez, K. McMurry, L. J. Meincke, M. Misra, B. L. Moseman, M. Mundt, A. C. Munk, R. T. Okinaka, B. Parson-Quintana, L. P. Reilly, P. Richardson, D. L. Robinson, E. Saunders, R. Tapia, J. G. Tesmer, N. Thayer, L. S. Thompson, H. Tice, L. O. Ticknor, P. L. Wills, P. Gilna, and T. S. Brettin, *J. Bacteriol.* **189** (2007) 3680.
11. D. Greenberg, J. Busch, P. Keim, and D. Wagner, *Investig. Genet.* **1** (2010) 4.
12. Anonymous, *Bacillus thuringiensis*. National Pesticide Telecommunications Network, Oregon State University (2000) <http://nptn.orst.edu>.
13. R. J. Doyle, F. Nedjat-Haiem, and J. S. Singh, *Curr. Microbiol.* **10** (1984) 329.
14. T. Koshikawa, M. Yamazaki, M. Yoshimi, S. Ogawa, A. Yamada, K. Watabe, and M. Torii, *J. Gen. Microbiol.* **135** (1989) 2717.
15. U. Husmark and U. Rönner, *J. Appl. Microbiol.* **69** (1990) 557.
16. U. Rönner, U. Husmark, and A. Henriksson, *J. Appl. Microbiol.* **69** (1990) 550.

17. S. Charlton, A. J. Moir, L. Baillie, and A. Moir, *J. Appl. Microbiol.* **87** (1999) 241.
18. C. Faille, C. Jullien, F. Fontaine, M. N. Bellon-Fontaine, C. Slomianny, and T. Benezech, *Can. J. Microbiol.* **48** (2002) 728.
19. M. Plomp, T. J. Leighton, K. E. Wheeler, and A. J. Malkin, *Langmuir* **21** (2005) 7892.
20. T. L. Buhr, D. C. McPherson, and B. W. Gutting, *J. Appl. Microbiol.* **105** (2008) 1604.
21. T. Y. Buhr, A. A. Young, D. McPherson, C. Hooban, A. Minter, D. Shegogue, D. Kota, V. Rozanski, M. Hammon, Sporicidal Efficacy Testing with Hot Humid Air to Evaluate the JBADS Decon System. NSWCDL Final Report: Spore Preparations, Environmental Chambers, and Heat Kill of *Bacillus Spores* (*B. anthracis* Ames, *B. anthracis*  $\Delta$ Sterne, *B. cereus* ATCC 4342, *B. thuringiensis* Al Hakam) Report submitted from N. S. W. Center-Dahlgren to Defense Threat Reduction Agency (2010).
22. T. L. Buhr, Hot Air Decontamination (HAD) of *Bacillus Spores*. *CBD S&T Conference* Orlando, FL (2010).
23. R. K. Hanson, *Proc. Combust. Inst.* **33** (2011) 1.
24. A. D. McCart, S. D. Gates, P. Lappas, J. B. Jeffries, and R. K. Hanson, *Appl. Phys. B* (2011) in press.
25. S. D. Gates, A. D. McCart, J. B. Jeffries, R. K. Hanson, L. A. Hokama, and K. E. Mortelmans, *J. Appl. Microbiol.* **111** (2011) 925.
26. J. B. Young and A. Guha, *J. Fluid Mech.* **228** (1991) 243.

